TRIUMF Experiment E614
Technical Note
Monte Carlo Summary Report to the E614 Collaboration

D.H. Wright, TRIUMF

10 April 1998

Abstract

This report summarizes the results of recent Monte Carlo studies concerning spectrometer design, effects of the solenoidal magnetic field and particle tracking. The design features addressed include: helium gap sizes, the use of DME buffer zones, whether or not to use field wires, whether or not to use PCs next to the stopping target, and the use of SiLi detectors. The magnetic field issues include: the use of correction coils at the entrance to the magnet and the importance of field inhomogeneities in longer versions of the spectrometer. Studies of particle tracking include attempts to restrict the momentum of the muon as a means to maximize the polarization. The present status of the Monte Carlo routines is also discussed.

DME Buffer Zones. Recent tests using the drift chamber prototype [1] have shown that the likely leak rate of gas from the helium gaps into the DME drift chamber is small enough that DME buffer zones will not be required. Further tests will be performed to decide whether or not such zones are required to prevent foil deflection under pressure, however for simulation purposes it is henceforth assumed that the DME buffer volumes and the extra mylar foils they require are absent. As shown in Figs. 1 and 2, this allows an improvement in both angle and momentum resolution.

Helium Gap Sizes in Spectrometer. It has been suggested [2] that instead of helium gaps of uniform length (4 cm) between drift chamber pairs in the spectrometer, gaps of 4 and 6 cm should be alternated. This has the advantage of removing the possibility that the wavelengths of certain helical tracks would coincide with the period of the chamber pairs, thus producing poor fits in the x or y projection. It would also substantially improve the momentum resolution by increasing the lever arm over which the track position is measured. This was verified by a Mone Carlo simulation of the new detector. The simulated spectrometer consisted of 26 drift chamber (DC) planes and 3 proportional chamber (PC) planes on each side of the stopping target. The 10 upstream-most DCs are closely packed, while the next 16 planes are grouped in 8 pairs, the center of each pair being spaced at alternating 4.8 and 6.8 cm distances. There were no PCs adjacent to the target, nor were there any DME buffer zones. Field wires were included. For this test, 50 and 20 MeV positrons were started at $z = 19.2$ cm and tracked through $z = 43.2$ cm for various initial angles. This distance covers the last five chamber pairs before the dense stack of drift chambers at the end of the spectrometer. These chambers represent the tracking unit or “slide” over which the resolution

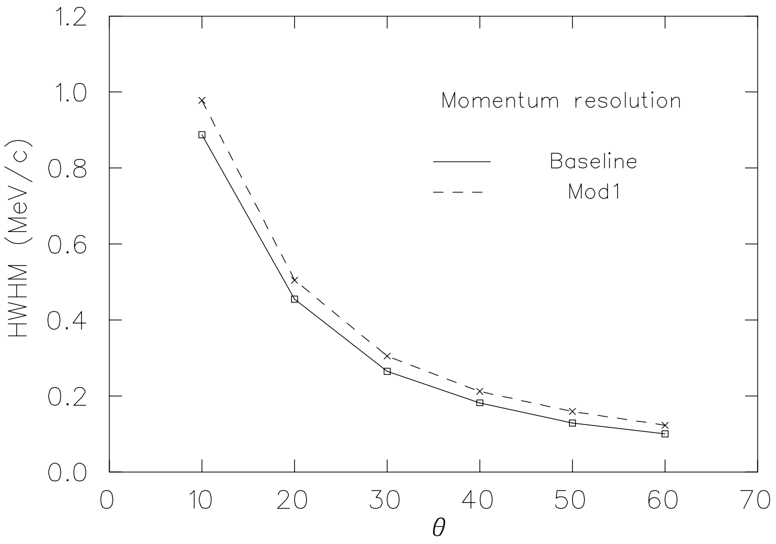

Figure 1: Momentum resolution for baseline spectrometer (solid line), and spectrometer modified to include DME buffer zones plus extra mylar foils (dashed line).

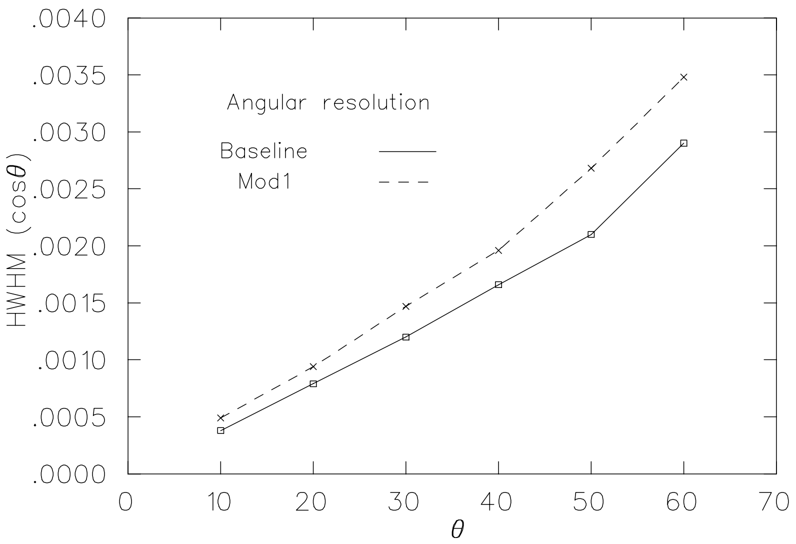

Figure 2: Angle resolution for baseline spectrometer (solid line), and spectrometer modified to include DME buffer zones plus extra mylar foils (dashed line).

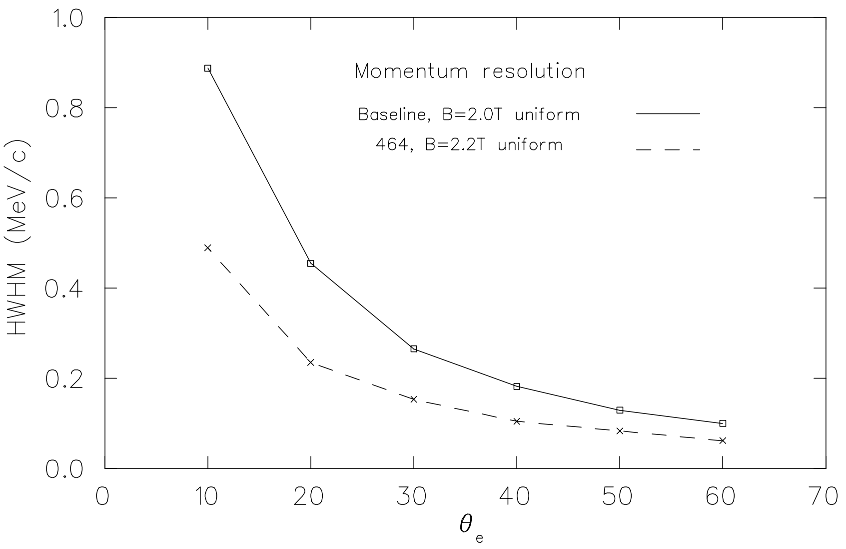

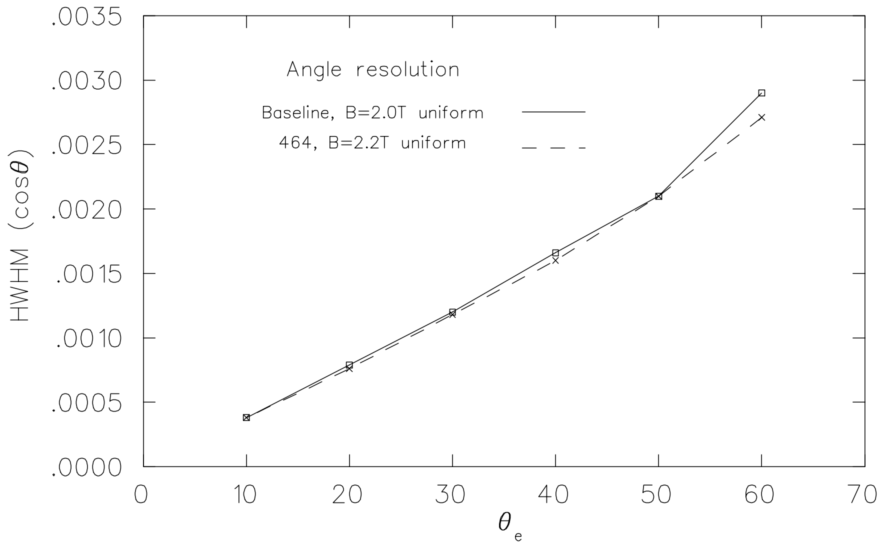

Figure 3: Top: momentum resolution for baseline spectrometer (solid line), and spectrometer modified to include alternating 4 and 6 cm helium gaps (464 option) (dashed line). Bottom: angle resolution for baseline spectrometer (solid line), and 464 option (dashed line).

is determined. The solenoidal field used was 2.2T, uniform throughout the detector. The baseline spectrometer had a uniform 4.8 cm separation between chamber pairs and used a slide consisting of four chamber pairs instead of five. The field used in the baseline analysis was a uniform 2.0T. The momentum and angle resolution for the two options is compared in Fig. 3. There is little difference in the angular resolution for the two cases. However, the difference in momentum resolution is substantial. Roughly half the difference is due to the increased average distance between chamber pairs. The other half is due to adding more planes, thus even more length, to the slide. There is almost no difference due to the increased field strength.

Two questions need to be settled before adopting this option: can a support cradle be designed to accommodate a detector which is now 12 cm longer, and does the longer detector extend far enough into the non-homogeneous field region to adversely affect the momentum and angle resolution?

Resolution in a Non-homogeneous Field. The second question was answered by repeating the above simulation using a non-homogeneous field map which reflects the expected magnet yoke and coil geometry. In this case the momentum and angle were reconstructed assuming a uniform field. As seen in Fig. 4 the difference in angle and momentum resolution is negligible. The only observable effect of the inhomogeneous field is a shift in the reconstructed positron momentum of 10 keV/c at 60° which increases to 20 keV/c at 10°. It is therefore recommended that the spectrometer design with alternating 4 and 6 cm spacers be adopted, provided it is mechanically feasible.

The Effect of Field Wires. It has so far been assumed that removing the 25.4 μm diameter copper field wires from the drift planes would reduce multiple scattering of positron tracks and especially high angle scattering due to the mass concentration of the wire. This was checked by simulation. The results, shown in Fig. 5 for 50 MeV/c positrons and Fig. 6 for 20 MeV/c positrons, indicate little if any difference when the wires were removed. Since the resolutions are given by half width at half maximum, this shows that the wires do not contribute significantly to small angle scattering. The effect on large angle scattering can be seen in Fig. 7, which shows the scattering angle, with and without field wires, due to the passage of a 20 MeV/c positron through 24 cm of the spectrometer (1 slide). In this case the magnetic field was turned off. An analysis of the histogram shapes shows that there are only about 10% more events with scattering angles greater than 1° when the field wires are included. For angles greater than 2° this rises to 39%, a value which remains nearly constant for the high-angle tail out to at least 20°. Of all events in the sample, the field wires are responsible for 2.8% with scattering angles greater than 1°, and 1.9% with angles greater than 2°. While the removal of field wires would certainly reduce the number of large-angle scatters, a reduction of only 2.8% would not justify possible difficulties with the no-field-wire design.

Proportional Chambers Adjacent to Target. The conclusion of Technical Note 5 [3] was that a pair of PCs on either side of and immediately adjacent to the stopping target would

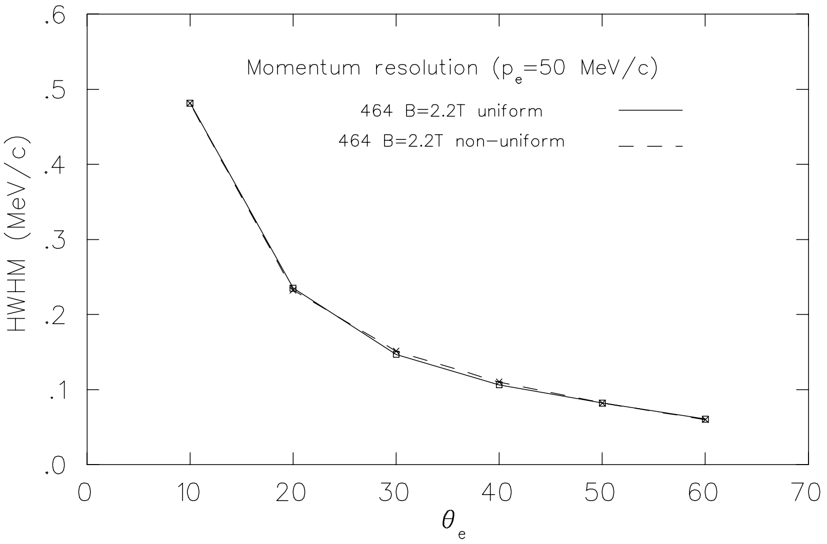

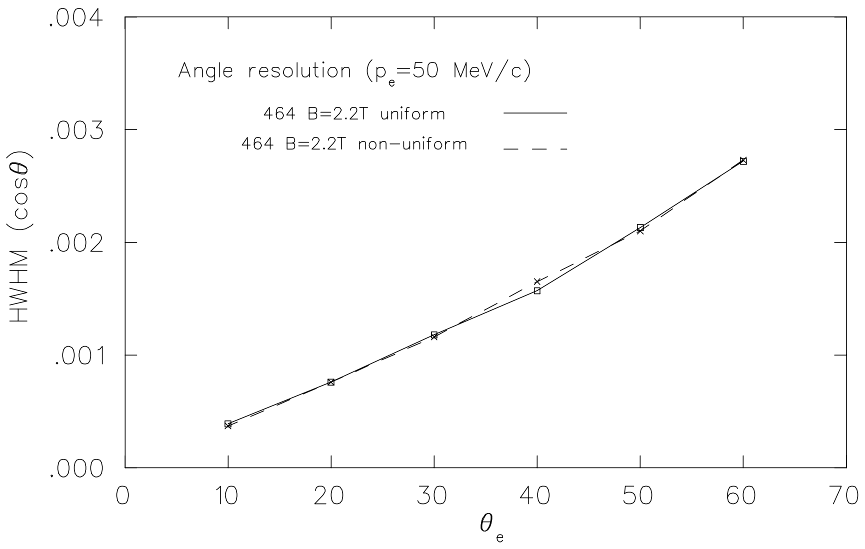

Figure 4: Top: momentum resolution for 50 MeV/c positrons in last slide of 464 spectrometer with uniform field (2.2T) (solid line), and with non-uniform, mapped field (2.2T at $z = 0$) (dashed line). Bottom: angle resolution for 50 MeV/c positrons in last slide of 464 spectrometer with uniform field (2.2T) (solid line), and with non-uniform, mapped field (2.2T at $z = 0$) (dashed line).

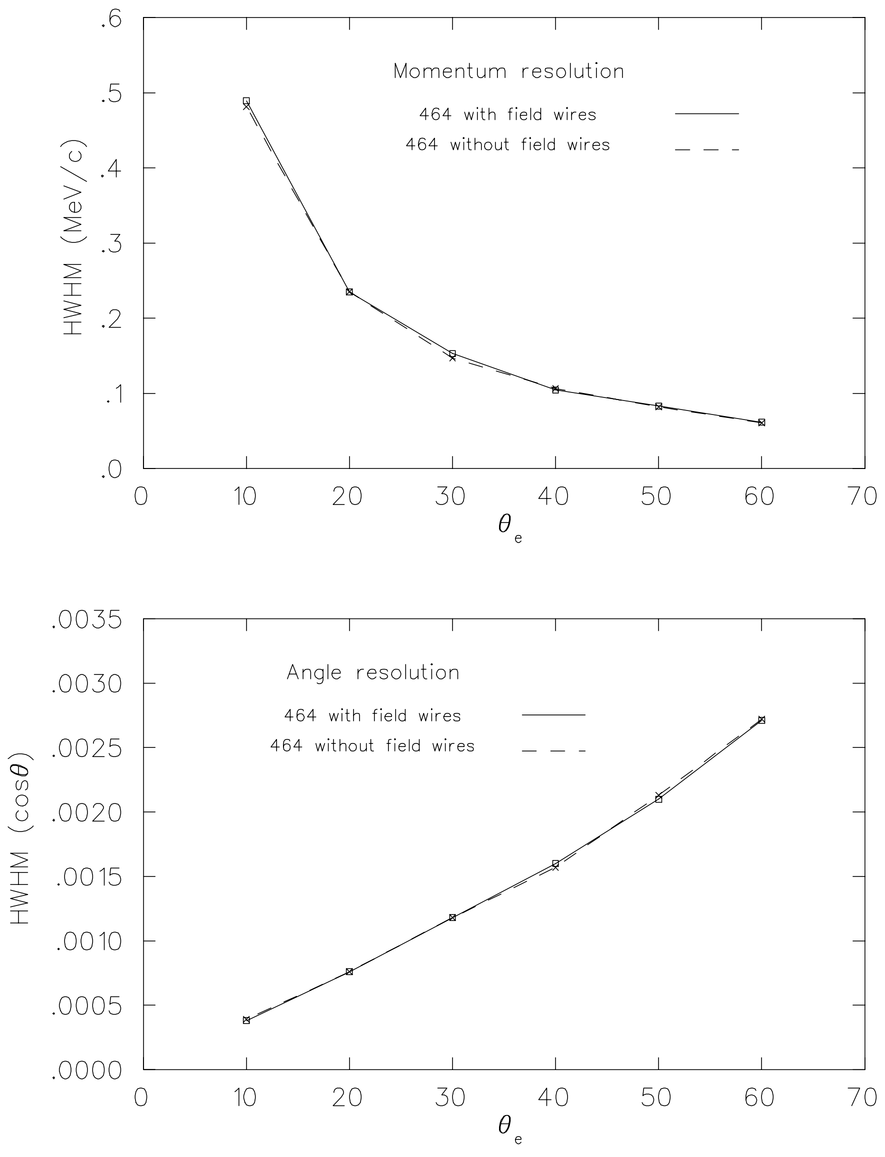

Figure 5: Top: momentum resolution for 50 MeV/c positrons with field wires (solid line), and without field wires (dashed line). Bottom: angle resolution for 50 MeV/c positrons with field wires (solid line), and without field wires (dashed line).

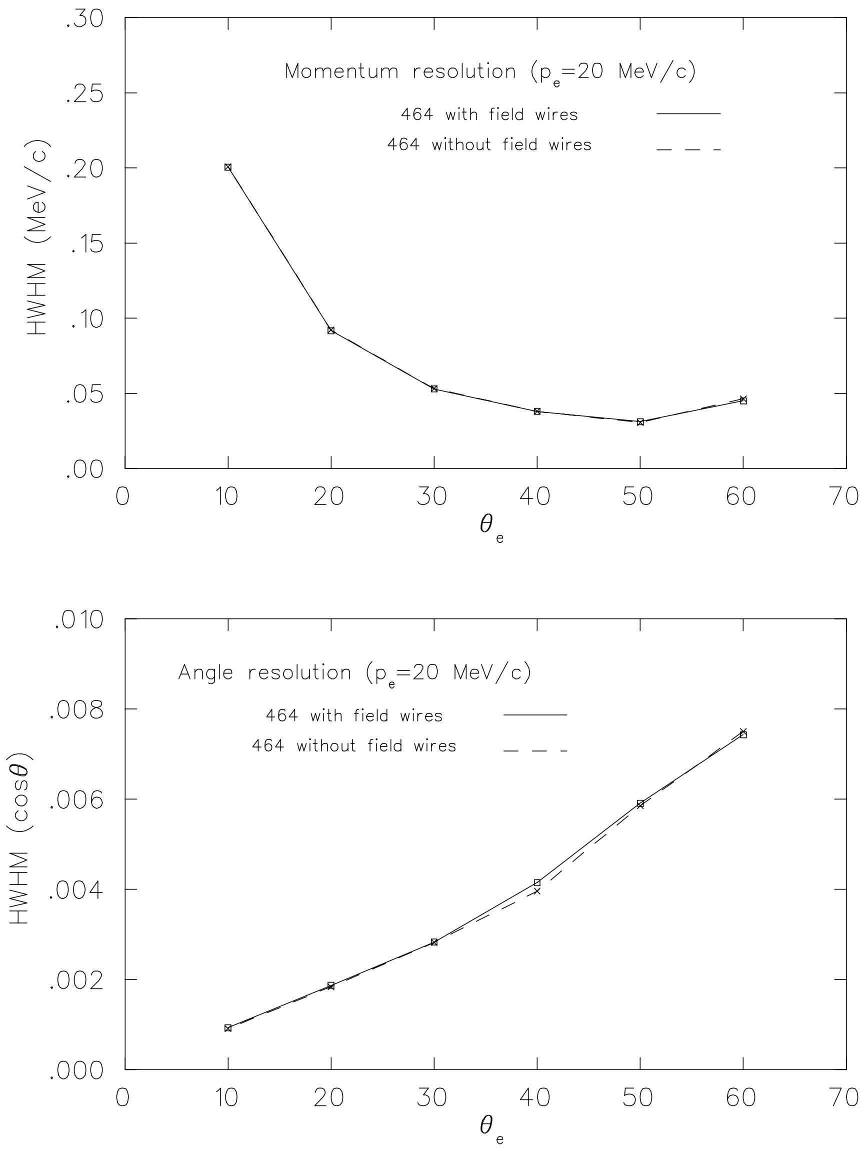

Figure 6: Top: momentum resolution for 20 MeV/c positrons with field wires (solid line), and without field wires (dashed line). Bottom: angle resolution for 20 MeV/c positrons with field wires (solid line), and without field wires (dashed line).

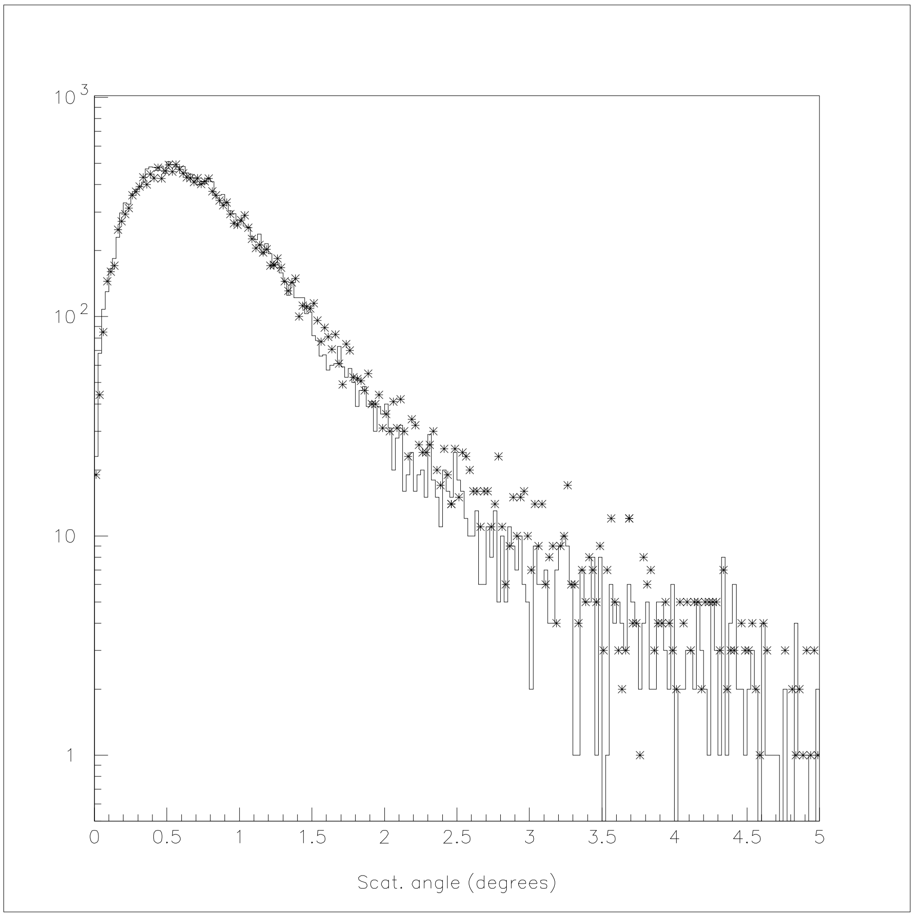

Figure 7: Scattering angle for 20 MeV/c positrons after passing through one slide without field wires (histogram), and with field wires (stars).

be sufficient to limit the systematic error in $P_\mu\xi$ due to depolarization in the PCs to a part in 10^4 or better. It could not be determined whether removing the central PCs and depending on muon tracking to locate stops would work, since that method depends on knowing the depolarization of muons in a 1 atm helium gas in a 2.2T longitudinal magnetic field. Because of experimental difficulties, no measurements exist for such large longitudinal fields and low pressures, although a recent calculation finds $P_{\mu He} = 0.98$ [4]. Before the no-PC option is chosen, a measurement in He gas must be performed to the level of 1% or better. The possibility of doing this measurement at TRIUMF is being studied, although problems due to the low density target have not been overcome, nor has a high field magnet of sufficient bore been located. The best option may be to use the E614 magnet for this measurement, provided it is ready for use well before the decision about the central PCs is made.

Muon Tracking in and out of the Fringe Field.

Given the importance of highly polarized muons to E614, methods were sought which could select the spin (and therefore the polarization) of muons at the stopping target. The first of these were discussed in Technical Note 7 [5]. An attempt was made to find a correlation between muon track parameters and the spin at the target and to select the spin either by collimating the beam or by cutting on the track parameters. It was found that a beam with a focus at the entrance to the solenoid (150 cm upstream of the stopping target) would suit this purpose better than a parallel beam. A focussed beam would have a smaller size at the point where the radial field is largest, thus reducing possible transverse spin components. This result depends on the field map at the solenoid entrance and on the beam rays used in the simulation. Each of these topics will be discussed in other summary reports. However, it is noted here that two different field maps, one with auxilliary field coils near the entrance and one without, were used in the spin studies with no difference between them discovered. The optimum location of the beam focus is shown in Fig. 8.

Two methods of restricting the spin were tried which look at muon tracks upstream of the solenoid fringe field. In the first method, two drift chamber pairs were placed just upstream of the fringe field where they measured the distance and angle of the incoming track from the beam axis, both of which correlate strongly with muon spin at the target in the absence of multiple scattering. However the multiple scattering in the added chambers weakens the correlation too much for the method to be useful. The second method would have removed tracks too far from the beam axis by using a slit or collimator at the focus of the muon beam ($z = -150$cm). However, the correlation between distance from the axis at the focus and spin at the target also turned out to be weak.

A more successful method [6] examines the muon tracks in the high field region but well away from the fringe field. In this case the track angle measured in the chambers of the baseline detector gives the z component of the momentum at the target. Hence the spin can be predicted, provided that multiple scattering along the path is not large. However the muon track angles are small, making their measurement from track fitting difficult. Extraction of the radius of the helix was found to be easier and to correlate with the spin at the target.

Using nine chamber pairs of the baseline spectrometer design, it was found that a cut on the fitted radius of the muon helix could enhance the polarization at the target, although the

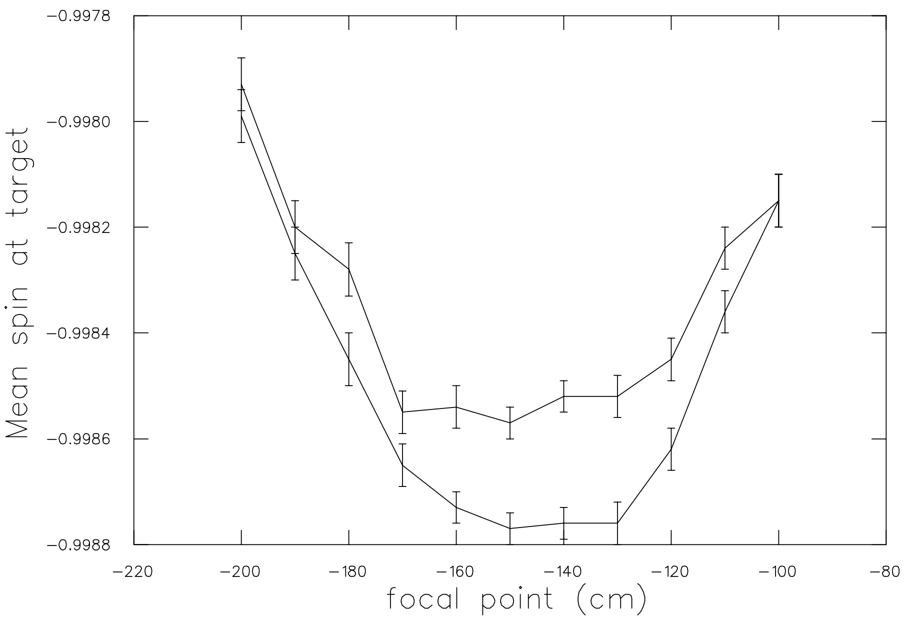

Figure 8: Mean muon spin at target vs. location of beam focus. Lower curve: mean spin at target. Upper curve: mean spin at target as predicted by track parameters fitted from muon detector points.

effect is not large as shown in Fig. 9. Adding more pairs to the fit made things worse due to increased multiple scattering. Part of the problem was due to the low energy and angle of the incident muon. The wavelength of the helices are typically 28 cm, too long for the spacings in the baseline spectrometer which was designed for positrons of higher energies and angles. For this reason a "muon detector" consisting of five chamber pairs spaced 7.0 cm apart was placed immediately upstream of the dense chamber array of the baseline spectrometer. Thus the entire wavelength is captured with a minimum of mass. The fitted helix radius from the muon detector was found to be correlated with the spin at the target, so that a cut on the radius significantly improved the mean of the spin distribution, as shown in Fig. 9.

The baseline spectrometer includes a SiLi counter for the identification of muons and possibly for trigger time definition. If the 10-plane muon counter is added, it could perform the identification function. A simulation of the sum of the energy loss in all the planes of the muon detector is shown in Fig. 10 for positrons, muons and pions of 29.7 MeV/c incident momentum. The muons are clearly separated from the positrons and pions, indicating that the muon detector stack can replace the SiLi detector for the identification task.

Status of the Monte Carlo Code. The machine LIN01 has been chosen as the official repository for E614 Monte Carlo code. Also, the latest version, 97a, of GEANT 3.21 is now being used. At present there are seven different geometry files corresponding to the various design options being considered. The current Monte Carlo version number, 0.25, reflects the unsettled state of affairs. Before an official version 1.0 is released, all or most of the above design decisions must be made. Future upgrades of the code will include second

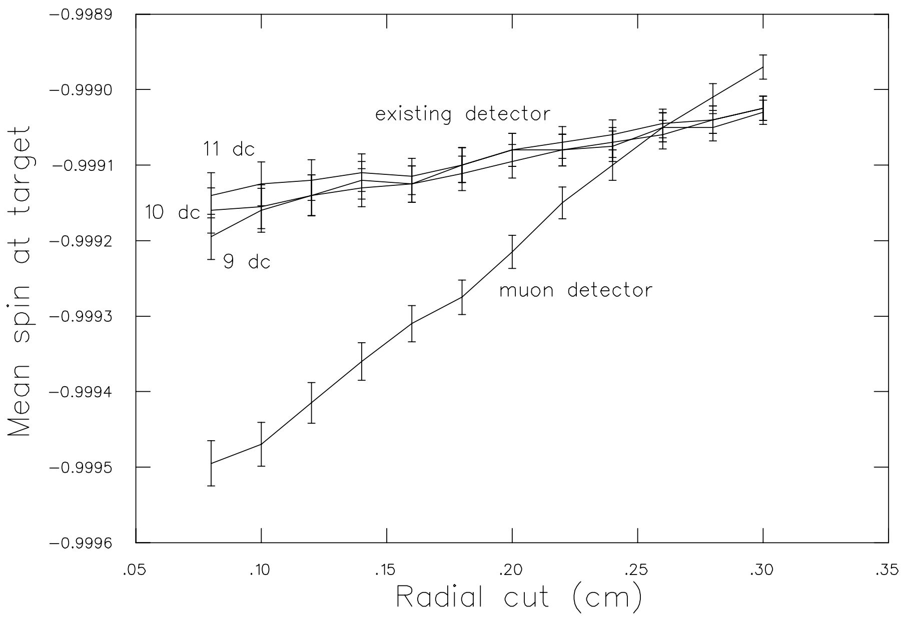

Figure 9: Mean muon spin at target vs. cuts on fitted muon helix radius. Upper curves: radius determined by fit using 9, 10 or 11 chamber pairs in baseline spectrometer. Lower curve: radius determined by using 5 chamber pairs in muon detector assembly.

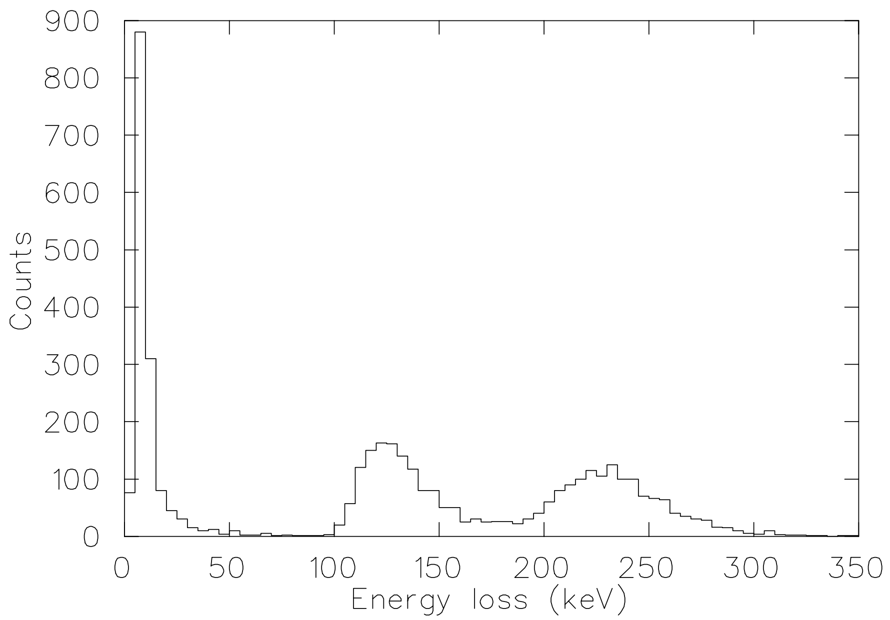

Figure 10: Energy loss (in keV) in 10 planes of DME by positrons, muons and pions (left,center and right, respectively) of 29.7 MeV/c.

order radiative corrections, the handling of secondary tracks and an event display for the full detector. The second order radiative corrections are being done in Russia and in Los Alamos and may be available in a year. A rudimentary event display using low level graphics exists, but further developement must await a standardized digitization package. As yet no work on secondary track handling has been done. It too will depend on the digitization.

The majority of the digitization code is complete and uses the GEANT user hooks GUSTEP, GUDIGI and GUOUT to generate data files. GUSTEP calls the routine STORE TRACK SEGMENTS which at entry and exit of each drift cell stores the particle position, momentum, time-of-flight and type. From this information the routines XPOCA and YPOCA reconstruct a helix and then find the point of closest approach to the sense wire. Currently the drift time is taken from the distance of closest approach but eventually this will be improved with the use of GARFIELD cell maps, charge cluster statistics, etc. The drift times are then fed to the routine SIMULATE 1877 TDC which codes the leading and trailing edge drift times into 32 bit words identical to those generated by the 1877 FBTDC. GUOUT writes the TDC words into YBOS banks which are organized according to event type and written out to disk or tape. Using this system positron helices were generated in both upstream and downstream ends of the spectrometer and at various energies. The events were successfully written to disk and then read and analyzed with a rudimentary helix track reconstruction routine. Before further developement of the digitization more work on YBOS bank orgainization must be done.

References

[1] R. MacDonald, E614 Technical Note # 6, December 1997.

[2] D.H. Wright, E614 Technical Note # 8, February 1998.

[3] D.H. Wright, E614 Technical Note # 5, November 1997.

[4] M. Senba, private communication, December 1997.

[5] R. MacDonald, E614 Technical Note # 7, January 1998.

[6] A.R. Parikh, report to E614 meeting, April 1998.